physica status solidi

pss

www.interscience.wiley.com

reprints

www.pss-rapid.com

www.pss-c.com

www.pss-b.com

www.pss-a.com

WILEY-VCH

REPRINT

Phys. Status Solidi A **206**, No. 9, 2098–2102 (2009) / **DOI** 10.1002/pssa.200982208

physica status solidi a
www.pss-a.com
applications and materials science

Correlation between thermally and optically stimulated luminescence in beta-irradiated undoped CVD diamond

V. Chernov*[,1], T. M. Piters[1], R. Meléndrez[1], S. Preciado-Flores[1], P. W. May[2], and M. Barboza-Flores[1]

[1] Departamento de Investigación en Física de la Universidad de Sonora, Apartado Postal 5-088, Hermosillo, Sonora 83190, México
[2] School of Chemistry, University of Bristol, Bristol BS8 1TS, UK

Received 7 March 2009, revised 10 July 2009, accepted 11 July 2009
Published online 21 August 2009

PACS 78.60.Kn, 81.05.Uw, 81.15.Gh

* Corresponding author: e-mail chernov@cajeme.cifus.uson.mx, Phone: +52 662 259 2156, Fax: +52 662 212 6649

The behaviour of afterglow (AG), thermoluminescence (TL) and infrared-stimulated luminescence (IRSL) in beta-irradiated chemical vapour deposition diamond is presented. The TL glow curve consists of four peaks with maxima at about 380, 430, 530 and 610 K. The AG decay is fitted by Becquerel's law with exponent close to 1, and correlates well with the thermal emptying of the traps responsible for the 380 K peak. Stimulation with IR light (830 nm) creates intense IRSL and destroys the 380, 430 and 530 K peaks. Illumination with shorter wavelength light also destroys the 610 K peak. The thermal cleaning procedure removes subsequently TL peaks, AG and IRSL. The AG signal decays together with the disappearance of the 380 K peak. The IRSL signal decays continuously with the removal of the 380, 430 and 530 K peaks. Traps responsible for the 610 K peak do not participate in the IRSL process.

1 Introduction Thermally stimulated luminescence (TL) as well as optically stimulated luminescence (OSL) have been proposed as suitable techniques for exploiting the dosimeter potential of diamond. TL and OSL created by radiation can also provide important information about intrinsic and impurity defects, and are widely used for the determination of kinetic parameters of electron and hole traps. Synthetic diamond made by chemical vapour deposition (CVD) has been extensively studied as a material for radiation detectors and TL dosimeters, mainly because of the unique properties that make it suitable for radiation dose measurements in biomedical applications. There are a number of reports in which the TL properties of CVD diamond films have been investigated (see, for instance, Refs. [1–3] and references therein). It has been also observed that some diamond samples exhibit luminescence emission immediately after irradiation, usually referred to as afterglow (AG) or long persistence luminescence. AG is caused by slow radiative recombination (phosphorescence) of electrons thermally released from filled shallow traps into the conduction band [4, 5]. Stimulation with infrared or visible light of CVD diamond that has previously been exposed to ionizing or UV radiation creates intense luminescence referred as OSL [6–10]. OSL is caused by interaction of the stimulating light with electrons trapped in optically active traps. Usually, these traps are also responsible for the TL peaks, so a correlation should exist between OSL and TL.

In this work, we report the behaviour of thermally and infrared (830 nm) stimulated luminescence (IRSL) in nominally undoped microcrystalline diamond films exposed to beta radiation, with the aim to establish the correlation between its TL and OSL properties.

2 Experimental All data reported in this work refer to the same film for comparison. Measurements on another film, grown under the same conditions, produced similar results. The film was grown for a total of 107 h on a monocrystalline silicon substrate using hot filament CVD and 1% CH_4/H_2 as process gases. The substrate was (100) oriented and had dimensions of about $0.5 \times 5 \times 5\,mm^3$. The thickness of the grown film was 53 μm and consisted of a polycrystalline layer with a columnar structure.

All measurements and procedures on the substrate covered with the diamond film were performed inside an adapted Risø TL/OSL reader (model TL/OSL – DA-15). In this device, a cup with the sample was placed on a rotating table

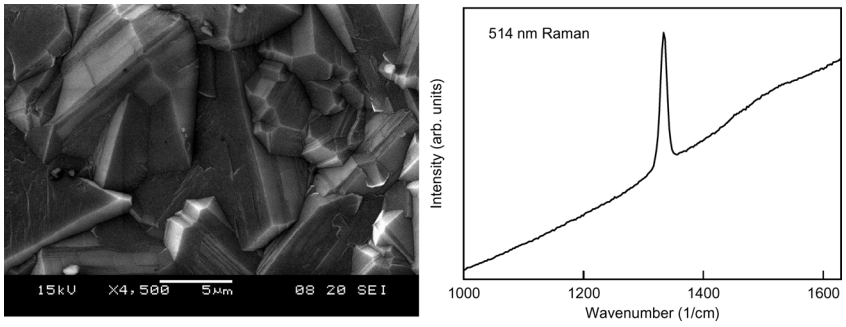

Figure 1 Characterization of the diamond film. Left: SEM micrograph. Right: Raman spectrum taken with 514 nm excitation.

and automatically moved to several positions at which measurements and procedures were performed. These included TL and OSL measurements, beta irradiations and optically bleaching procedures. The device was equipped with a 33 mCi ^{90}Sr–^{90}Y source for the beta irradiations, with an IR laser (830 nm, ~0.4 W at 100% power) for the infrared stimulation, a heater for thermal stimulation and a photomultiplier tube (Electron Tubes Inc., type 9235QB) for measurements of stimulated luminescence. According to the Riso devise specifications, the indicated activity of the beta source corresponds to a dose rate of about 300 Gy/h in quartz. The stopping powers (in MeV cm^2/g unit) of diamond and quartz are closer than 5% for electron energies between 0.3 and 2.5 MeV so that the absorbed dose rate in diamond could be taken equal to that in quartz [11]. For the optical bleaching, the original device was adapted by the introduction of the end of an optical fibre at one of the possible sample positions. The other end of the fibre was coupled to the exit slit of a motorized monochromator (Kratos, model GM252). The entrance slit of the monochromator was coupled to an automated home-built shutter, which was itself coupled to an Oriel lamp housing (model 66921) equipped with a xenon arc lamp (Oriel, model 6262) operating at 300 W. The bandwidth of the bleaching light was about 15 nm for the entrance and exit slit values of 5 mm. Optical bleaching with the xenon lamp, beta irradiations and IRSL readouts were all performed at room temperature (RT). The heating rate of TL readouts was 2 K/s. To protect the photomultiplier all luminescence measurements were performed with a Schott BG-39 bandpass filter (transmission 330–620 nm) in front of the photomultiplier. The TL/OSL reader device, the shutter and the monochromator were interfaced to a computer from where they were controlled by a bespoke computer program. The computer program allowed subsequent experiments including irradiation, bleaching, TL and or OSL measurements to be performed automatically.

3 Results

3.1 Sample characterization The surface morphology of the grown diamond films was examined by scanning electron microscopy (SEM). Figure 1 (left) shows a micrograph of the diamond film surfaces. The film covered the entire surface of the substrate and exhibited polycrystalline morphology. The film was composed of sharp, well-faceted microcrystallites ranging in size from about 1 to 10 μm, with many twinned crystallites and no obvious preferential orientation. The Raman spectrum of the film (Fig. 1, right) exhibits a sharp band at 1332 cm^{-1} attributed to the first-order phonon mode for diamond, which is the characteristic of a good quality diamond.

3.2 Afterglow, thermally and optically stimulated luminescence The TL glow curves of the CVD diamond film are depicted in Fig. 2 (left). The film was irradiated with beta radiation in 20–400 Gy dose range. At low dose the glow curve exhibits two separate TL peaks with maxima at about 380 and 610 K and an intermediate part between with unstructured TL. All of the three parts of the TL curve grow with increasing dose, but the intermediate part grows faster and becomes dominant at doses higher than 100 Gy. Our measured TL high dose responses are comparable to other studies [12–15] and higher to many works that report TL saturation at few Gy.

After irradiation with beta rays at RT the diamond film exhibited luminescence emission that is usually referred to as persistent luminescence or AG. Figure 2 (right) shows

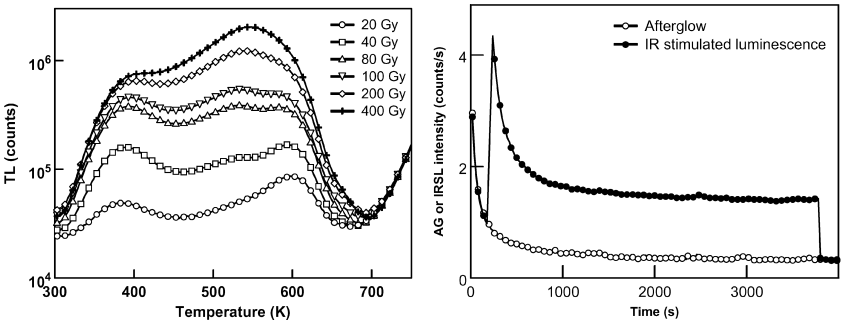

Figure 2 Left: TL glow curves of the diamond film irradiated with the indicated beta doses. Right: AG and IRSL decay curves recorded immediately after beta irradiation with 30 Gy.

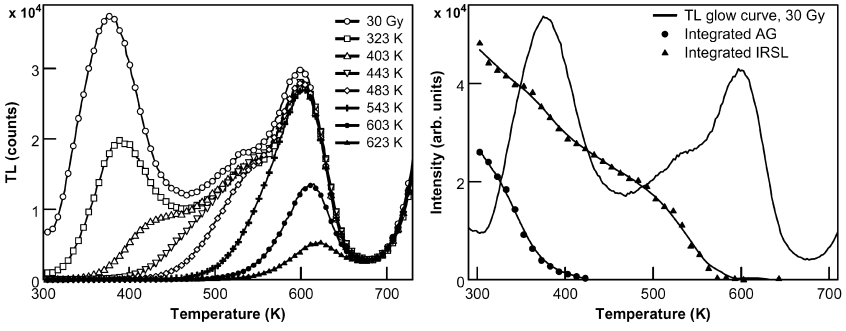

Figure 3 Left: TL glow curves recorded after beta irradiation (the upper curve) and after beta irradiation followed by preheats up to the indicated temperatures (thermal cleaning). Right: Dependences of integrated AG and IRSL signals (points) on preheat temperature.

the AG decay curve recorded immediately after the end of irradiation. The curve gradually decreases with time to the background level. The AG intensity increases as irradiation dose increases but the shape of the AG decay curves did not change significantly. The decay curve is fitted well by the phenomenological Becquerel's law [16]

$$I_{\mathrm{AG}}(t) = \frac{I_0}{(1 + t/\tau)^a}, \tag{1}$$

where the exponent a is close to 1 and τ is ~60 s. This kind of decay, with $a \sim 1$, is typical for second-order kinetics.

Figure 2 (right) also shows the effect of stimulation with 830 nm light on the luminescence of the beta-irradiated diamond film. After irradiation the film exhibits intense AG due to thermal emptying of traps. When the IR stimulation is switched on, the luminescence intensity increases sharply due to additional emptying of the traps by light. Further stimulation decreases the luminescence that decays faster than AG. Once the stimulation light is switched off, the luminescence intensity drops down rapidly to the background level (it should be mentioned that the background level depends on the IR stimulation power).

3.3 Effect of thermal cleaning on TL, AG and IRSL

A thermal cleaning procedure was carried out to clarify the structure of the glow curves. This procedure consisted of the following repeated steps: beta irradiation with 30 Gy, preliminary TL readout up to preheat temperature, cool down to RT, second TL readout up to 753 K (preheated glow curves), cool down to RT. The preheat temperature was changed from 303 to 663 K with step size of 20 K. Figure 3 (left) shows the initial and preheated TL glow curves of the diamond film subjected to beta irradiation with 30 Gy. The preheated glow curves show the typical subsequent disappearance of the TL peaks. The disappearance of the first peak is accompanied by the shifting of its maximum towards higher temperatures. This indicates (together with the symmetric appearance of the peak) that this peak behaves according to second-order kinetics. Further increasing of the preheat temperature reveals that the glow curve between 430 and 530 K consists of at least two peaks with maxima at about 470 and 550 K. The last TL peak has a maximum at ~610 K. Its maximum also moves a little towards higher temperatures with increasing preheat temperature. So, either this peak obeys non-first-order kinetics, or an additional TL peak with maximum at about 650 K exists. Hereafter, suppose that the TL curve of the diamond film consists of four peaks with maxima at 380, 430, 530 and 610 K, we will use these temperatures to specify these peaks.

The effect of the thermal cleaning on the AG and IRSL has also been studied to determine the traps responsible for the AG and IRSL. The procedure was similar to that described previously, and consisted of the following repeated steps: first beta irradiation with 30 Gy, preliminary TL readout up to a preheat temperature, cool down to RT, AG measurements at RT during 240 s (preheated AG), second TL readout up to 753 K (preheated and storage-affected glow curve), cool down to RT, second beta irradiation with 30 Gy, preliminary TL readout up to specified preheat temperature, cool down to RT, IRSL measurements at RT during 240 s (preheated IRSL), second TL readout up to 753 K (preheated and IRSL-affected glow curve) and finally cool down to RT. The preheat temperature was changed from 303 to 663 K with a step size of 10 K.

The effect of the thermal cleaning on AG and IRSL signals is shown in Fig. 3 (right) where the TL glow curve recorded immediately after beta irradiation is also presented. In the case of AG, the points are the integrated preheated AG with subtracted background ($\mathrm{AG_{pre}}$). The measured IRSL signal at RT consists of luminescence stimulated both by IR light and by heat (AG), so the differences between integrated preheated IRSL with subtracted background ($\mathrm{IRSL_{pre}}$) and $\mathrm{AG_{pre}}$ were presented as the IRSL points.

Figure 3 (right) gives clear evidence that AG is related directly with the 380 K peak. Among various mechanisms responsible for AG the simplest is due to the radiative recombination of electrons thermally released from filled traps into the conduction band. In our case, the 380 K peak is the most unstable at RT (see below); so the AG process in the beta-irradiated diamond film is the phosphorescence process determined by the thermal emptying of the traps responsible for the 380 K peak.

As in the case of AG, the preliminary heating also destroys IRSL. The destruction of IRSL with increasing preheat temperature is monotonic, but exhibits three poorly defined regions: up to 400 K, between 400 and 500 K, and for preheating temperatures, higher than 500 K. For these regions, the IRSL decay is mainly caused by the thermal decay of 380, 430, and 530 K peaks, respectively. The IRSL is fully absent in the diamond film preheated up to 600 K and

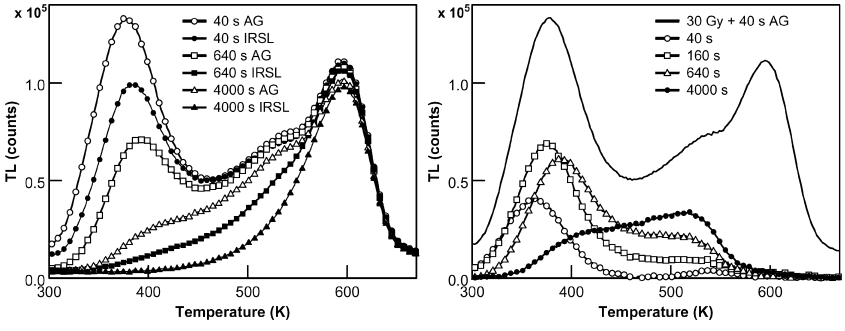

Figure 4 Effect of AG and IRSL readout TL. Left: TL glow curves recorded after beta irradiation with 30 Gy followed by AG (open markers) or IRSL (solid markers) readouts during indicated time. Right: The difference curves between samples recorded after AG and IRSL readouts with the indicated readout time. The solid line is the upper curve from the left figure.

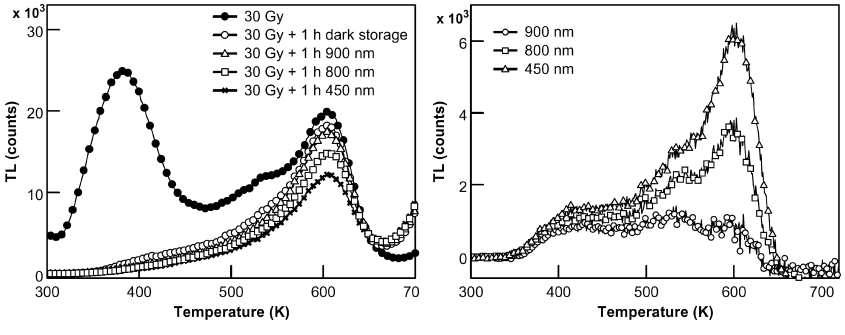

Figure 5 Effect of light illumination on TL. Left: TL glow curves recorded after beta irradiation followed by the indicated treatments. Right: The difference curves between the curve recorded with 1 h dark storage and the curve recorded with 1 h light illumination of indicated wavelengths.

to higher temperatures where only the 650 K peak exists. So the 830 nm light cannot release trapped electrons from the traps of the 650 K peak.

3.4 Bleaching of TL by IR and visible light Additional information about the correlation between TL and IRSL can be obtained from the optical bleaching of TL. For this, two types of optical bleaching were carried out, first with the IRSL readouts and then with the Xenon lamp. Because of the TL decay during long time storage (fading), each bleaching measurement was repeated with zero light intensity.

The bleaching with the IRSL readouts consisted of the following repeated steps: first beta irradiation with 30 Gy, AG measurements at RT during 240 s, TL readout up to 753 K (dark-storage-affected glow curve), cool down to RT, second beta irradiation with 30 Gy, IRSL readout at RT during 240 s, TL readout up to 753 K (IRSL-affected glow curve), cool down to RT. The readout time of AG and IRSL was 20, 40, 80, 160, 320, 640, 1000, 2000 and 4000 s. Figure 4 (left) shows the dark-storage and IRSL-affected TL glow curves. AG readout or fading changes the TL glow curve shape drastically. The main change is caused by the decaying of the 380 K peak, which completely disappears after 1 h of dark storage. The decay of the other peaks is not so pronounced but nevertheless noticeable. It is a little strange, especially for the 610 K peak, whose traps have too high activation energy to be emptied at RT.

Stimulation with 830 nm light (IRSL readout procedure) causes additional removal of the TL peaks. Figure 4 (right) shows the difference curves between the dark-storage- and IRSL-affected TL glow curves. These curves present the components of TL glow curves, which are bleached by 830 nm light illumination. It can be seen that the 830 nm light only destroys the TL between 300 and 600 K, which correspond to the 380, 430 and 530 K peaks and that the 610 peak is left unaffected. Thus, the IRSL signal is related to the release of electrons by 830 nm light from the traps responsible for the 380, 430 and 530 K peaks.

The bleaching with the xenon lamp consisted of the following repeated steps: beta irradiation with 30 Gy, illumination with light of selected wavelength at RT during 1 h, TL readout up to 753 K (light-affected glow curve) and cool down to RT. The wavelength was changed from 900 to 450 nm with a step size of 50 nm. Before the bleaching measurements, the TL of the film that had been beta irradiated with 30 Gy followed by 1 h dark storage was recorded. Figure 5 (left) shows the light-affected TL glow curves as well as the glow curve recorded without light stimulation. The effects of bleaching with the xenon lamp are similar to those of the IRSL readout. The only difference that was observed is the pronounced removal of the 610 K peak by visible light. This means that all the TL traps are optically active and can be ionized by light. The optical ionization threshold energy of the traps responsible for the 610 K peak is close to 1.5 eV (the energy of the IRSL stimulation light). The thresholds of the 380, 430 and 530 K peak traps are lower.

4 Conclusions The TL glow curve of the investigated beta-irradiated CVD diamond samples consists of four overlapped peaks. The first pronounced TL peak obeys second-order kinetics. The peak maximum (at 380 K if recorded immediately after beta irradiation) moves towards higher temperatures with dark storage (fading) or preliminary heating. The other TL peaks have maxima at about 430, 530 and 610 K, but their nature needs to be clarified by further investigation.

Immediately after irradiation, the sample exhibits pronounced AG (phosphorescence) caused by thermal emptying of the traps responsible for the 380 K peak. Stimulation with IR light (830 nm) creates IRSL and removes the 380, 430 and 530 K peaks. Illumination with shorter wavelength light also removes the 610 K peak. The thermal cleaning procedure subsequently removes TL peaks, AG and IRSL. The AG signal decays together with the removal of the 380 K peak. The IRSL signal decays continuously with the removal of the 380, 430 and 530 K peaks. Traps responsible for the 610 K peak do not participate in the IRSL process.

Acknowledgements The financial support from CONACyT (Mexico) Grant Nos. 83536 and 82765, and SEP (Mexico) is greatly acknowledged.

References

[1] J. Krása, B. Marczewska, V. Vorlíček, P. Olko, and L. Juha, Diamond Relat. Mater. **16**, 1510–1516 (2007).
[2] M. Barboza-Flores, R. Meléndrez, V. Chernov, M. Pedroza-Montero, S. Gastelum, and E. Cruz-Zaragoza, Mater. Res. Soc. Symp. Proc. **1039**, 145–154 (2008).
[3] C. Manfredotti, Diamond Relat. Mater. **14**, 531–540 (2005).
[4] L. M. Apátiga, V. M. Castaño, and F. Alba, J. Mater. Sci., Mater. Electron. **9**, 473 (1998).
[5] M. Barboza-Flores, M. Schreck, S. Preciado-Flores, R. Meléndrez, M. Pedroza-Montero, and V. Chernov, Phys. Status Solidi A **204**, 3047–3052 (2007).
[6] M. Barboza-Flores, R. Meléndrez, J. A. N. Gonçalves, G. M. Sandonato, V. Chernov, E. Cruz-Zaragoza, J. D. Ochoa-Nuño, R. Bernal, C. Cruz-Vázquez, and F. Brown, Phys. Status Solidi A **201**, 2548–2552 (2004).
[7] J. A. N. Gonçalves, G. M. Sandonato, R. Meléndrez, V. Chernov, M. Pedroza-Montero, E. De la Rosa, R. A. Rodríguez, P. Salas, and M. Barboza-Flores, Opt. Mater. **27**, 1231–1234 (2005).
[8] M. Pedroza-Montero, V. Chernov, B. Castañeda, R. Meléndrez, J. A. N. Gonçalves, G. M. Sandonato, R. Bernal, C. Cruz-Vázquez, F. Brown, E. Cruz-Zaragoza, and M. Barboza-Flores, Phys. Status Solidi A **202**, 2154–2159 (2005).
[9] S. Preciado-Flores, M. Schreck, R. Meléndrez, V. Chernov, M. Pedroza-Montero, and M. Barboza-Flores, Phys. Status Solidi A **203**, 3173–3178 (2007).
[10] M. Benabdesselam, P. Iacconi, L. Trinkler, B. Berzina, and J. E. Butler, Radiat. Prot. Dosimetry **119**, 390–393 (2006).
[11] On-line calculation with the ESTAR program of NIST (National Institute of Standards and Technology, USA). www.physics.nist.gov/PhysRefData/Star/Text/ESTAR.html.
[12] C. Descamps, D. Trompson, M. J. Guerrero, C. Mer, E. Rzepka, M. Nesladek, and P. Bergonzo, Diamond Relat. Mater. **15**, 833 (2006).
[13] C. Furetta, G. Kitis, A. Brambilla, C. Jany, P. Bergonzo, and F. Foulon, Radiat. Prot. Dosimetry **84**, 201 (1999).
[14] M. Benabdsselam, P. Iacconi, D. Briand, and A. Berkane-Krachaï, J. Appl. Phys. **88**, 4648 (2000).
[15] F. Wrobel, M. Benabdesselam, P. Iacconi, and F. Mady, Radiat. Prot. Dosimetry **119**, 115 (2006).
[16] M. N. Berberan-Santos, E. N. Bodunov, and B. Valeur, Chem. Phys. **317**, 57–62 (2005).

